Supporting Information for:

Hexa-*peri*-hexabenzocoronene decorated with an allenylidene ruthenium complex – almost a flyswatter

Rebecca Lorenz,[a] David Reger [b], Ruth Weller [ac], Norbert Jux [*b] and Nicolai Burzlaff [*a]

a Department Chemistry and Pharmacy, University of Erlangen-Nuernberg, Egerlandstr. 1, 91058 Erlangen, Germany.

b Department Chemistry and Pharmacy, University of Erlangen-Nuernberg, Nicolaus-Fiebiger-Str. 10, 91058 Erlangen, Germany.

c Fb. 15 – Chemie, Philipps-University Marburg, Hans-Meerwein-Straße 4, 35032 Marburg, Germany.

Crystallographic Details

Single crystals suitable for X-ray diffraction analysis of **8** were obtained by vapor diffusion of *n*-pentane into a solution of **8** in acetone The structure determination was carried out on a *Rigaku Oxford Diffraction* (formerly Agilent) *SuperNova A S2* (Dual) diffractometer using an Atlas S2 CCD detector and Mova (Mo) X-ray sources (Mova, Mo-Kα: λ = 0.71073 Å). Single crystals were coated with perfluoropolyether, picked with a loop and immediately mounted in the nitrogen cold gas stream of the diffractometer. Images were interpreted and integrated with the program CrysAlisPro (Agilent Technologies).[1] The structures were solved by using direct methods and refined with full-matrix least squares against F^2 (ShelXT[2–4] as part of Olex2[5]). The hydrogen atoms were included in their calculated positions and refined in a riding model. The structure pictures were prepared with the program DIAMOND 2.1e.[6,7] If atoms show disorder, the atoms with higher occupancy were chosen for representation.

The PF_6^- anion of the complex is disordered and occupies three different sites with occupancies of 0.4, 0.3 and 0.3. The unit cell contains most likely four acetone solvent molecules. Two of these are slightly disordered and one is severely disordered sharing at least one site with the disordered PF_6^- anion. Thus, the 0.4 occupancy of the anion defines the 0.6 occupancy/number of the forth acetone molecule in the refined model. Unfortunately, the last part(s) of the severely disordered acetone could not be resolved. This resulted in 3.6 acetone molecules in the refined model.

CCDC 2005956 contains the supplementary crystallographic data for this paper. These data can be obtained free of charge from The Cambridge Crystallographic Data Centre via www.ccdc.cam.ac.uk/structures.

*Table 1 Details for structure determination of **8**.*

empirical formula	$C_{112}H_{97}F_6P_3Ru \times 3.6\ C_3H_6O$
formula mass [g mol^{-1}]	1963.14
crystal color/habit	clear reddish brown plates
crystal system	triclinic
space group, Z	$P\bar{1}$, 2
a [Å]	14.9819(3)
b [Å]	19.1809(4)
c [Å]	20.0515(4)
α [°]	75.2303(17)
β [°]	70.2676(18)
γ [°]	67.3264(19)
V [Å^3]	4952.66(19)
Θ [°]	2.8740 to 29.1220
H	−18 to 18
K	−23 to 23
L	−25 to 25
F(000)	2058.0
μ (Mo-K_α) [mm^{-1}]	0.71073
crystal size [mm]	0.353 × 0.23 × 0.112
D_{calcd} [g cm^{-3}], *T* [K]	1.316, 100.01(10)

reflections collected	122139
independent reflections	20211
obs. Reflections, $I>2\sigma I$	16792
parameter	1579
weight parameter *a*	0.0783
weight parameter *b*	7.2482
R_1 (observed)	0.0541
R_1 (overall)	0.0683
wR_2 (observed)	0.1425
wR_2 (overall)	0.1552
diff. peak/hole [e/Å]	1.206 / −0.911
goodness-of-fit on F^2	1.052

References:

[1] Agilent technologies, *CrysAlis Pro*, Oxfordshire England, **2014**.

[2] G. M. Sheldrick, *Acta Cryst.* **2015**, *A71*, 3.

[3] G. M. Sheldrick, *Acta Cryst.* **2015**, *C71*, 3.

[4] O. V. Dolomanov, L. J. Bourhis, R. J. Gildea, J. A. K. Howard, H. Puschmann, *J. Appl. Crystallogr.* **2009**, *42*, 339.

[5] O. V. Dolomanov, L. J. Bourhis, R. J. Gildea, J. A. K. Howard, H. Puschmann, *J. Appl. Crystallogr.* **2009**, 339.

[6] K. Brandenburg, M. Berndt, *Diamond - Visual Crystal Structure Information System*, Crystal Impact Gbr, Bonn (Germany), **1999**.

[7] W. T. Pennington, *J. Appl. Crystallogr.* **1999**, *32*, 1028

Appendix:

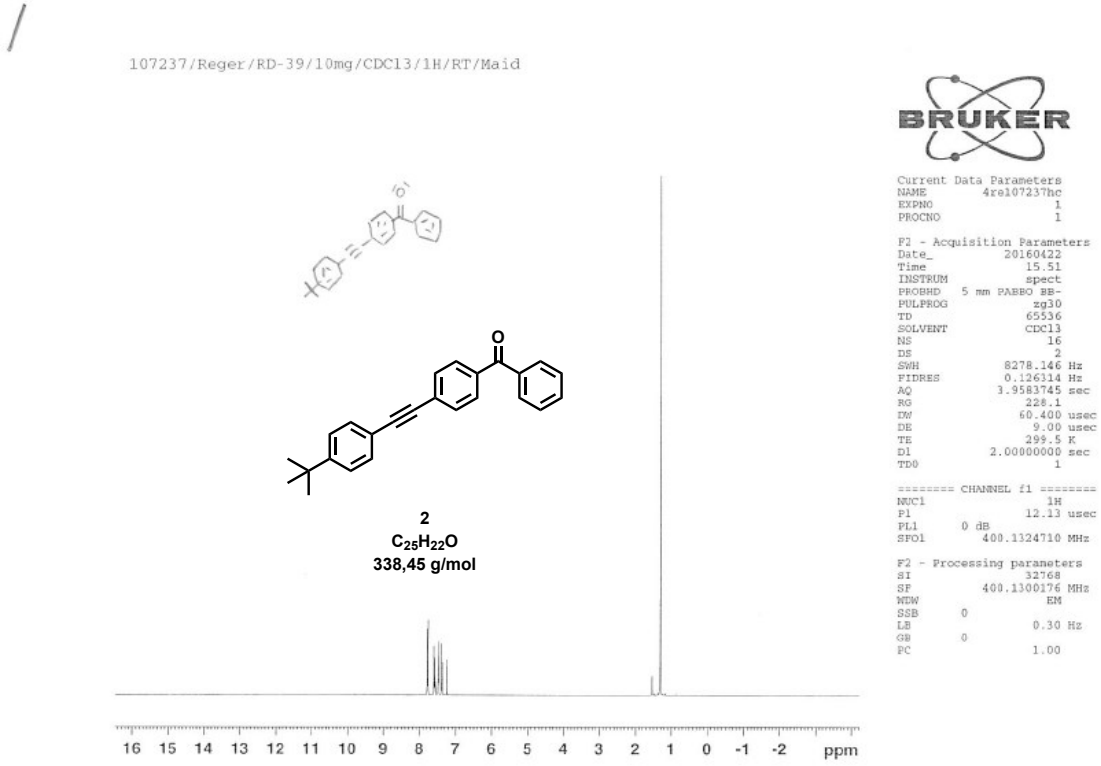

Figure S1: ^{1}H NMR spectrum of 2 ($CDCl_3$, 400 MHz; rt.).

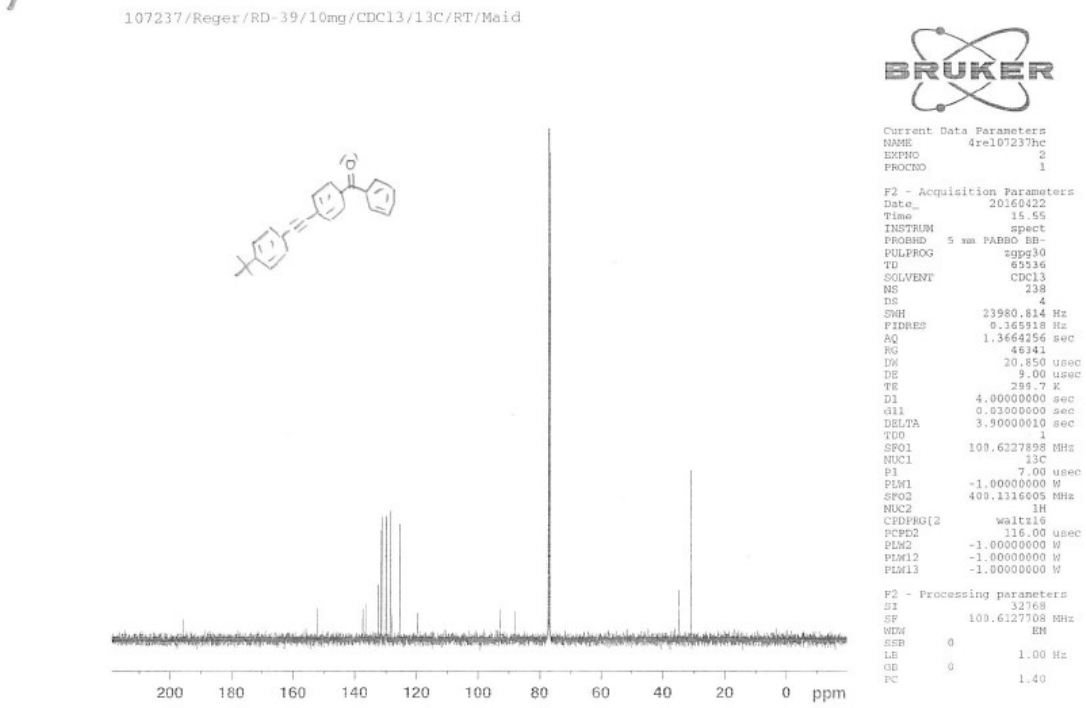

Figure S2: $^{13}C\{^{1}H\}$ NMR spectrum of 2 ($CDCl_3$, 100 MHz; rt.)

.

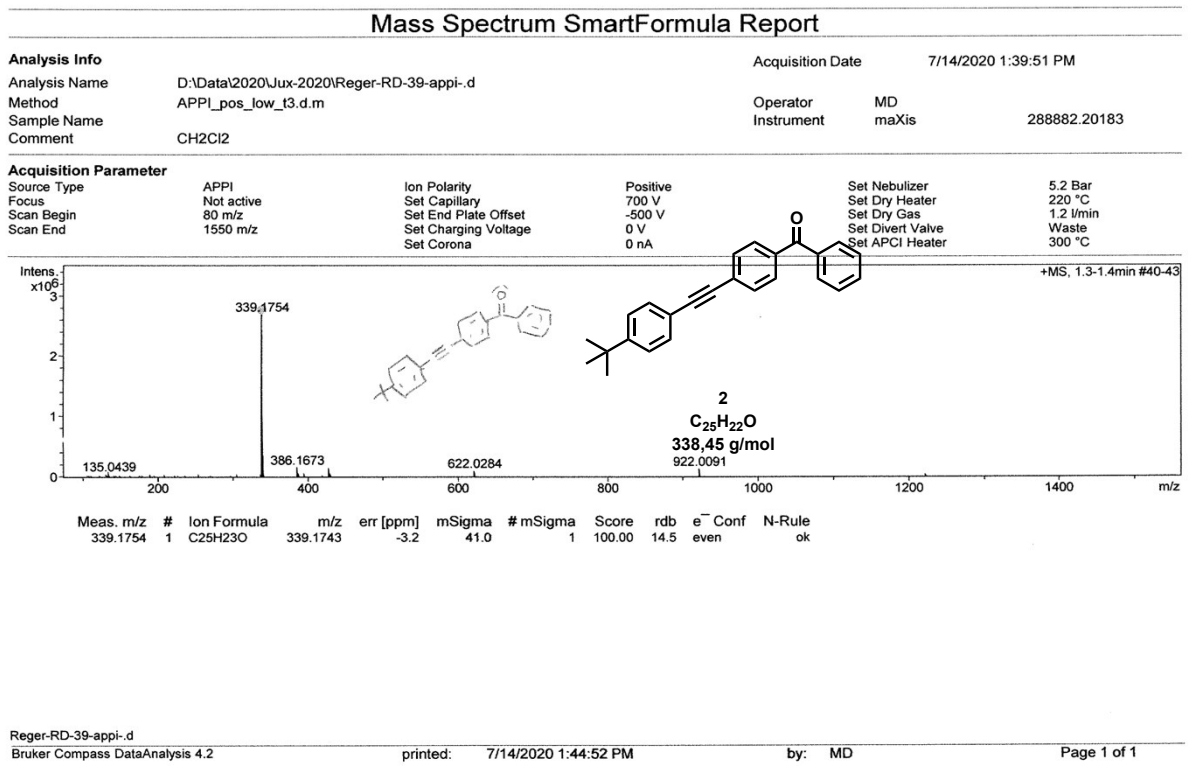

*Figure S3. HRMS spectrum of **2** (APPI, CH_2Cl_2) (overview).*

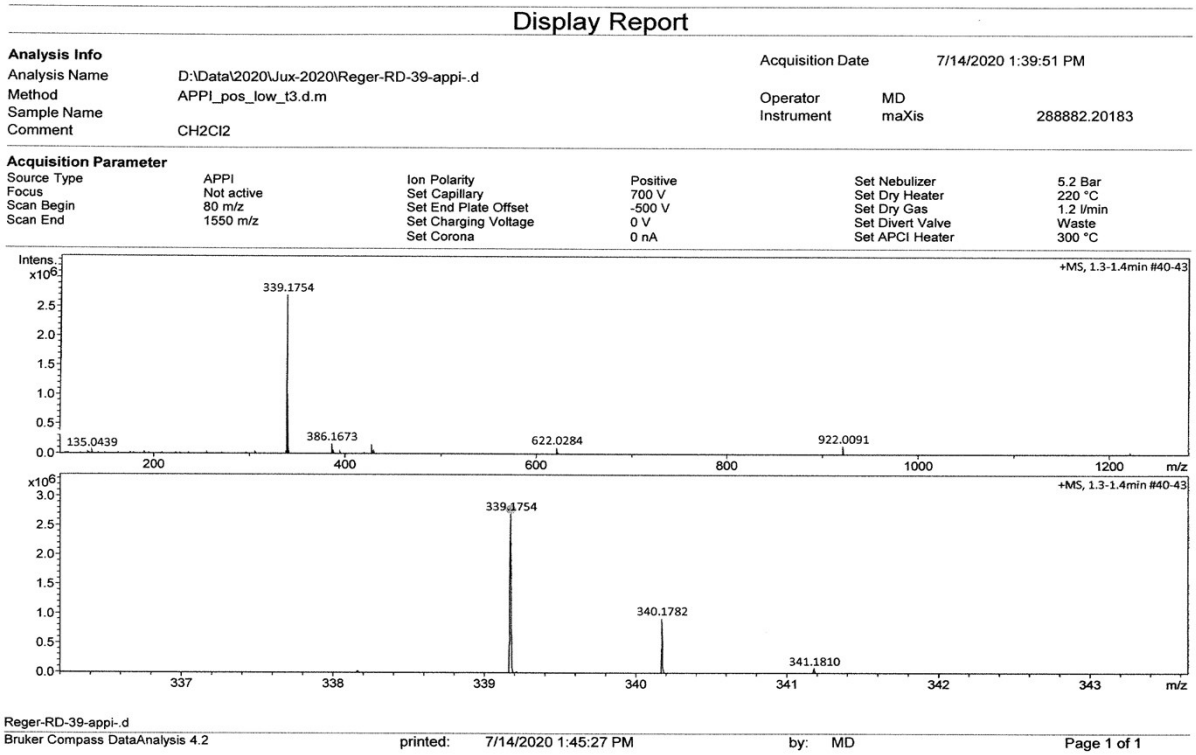

*Figure S4. HRMS spectrum of **2** (APPI, CH_2Cl_2). Top: Overview; Bottom: Zoom in on the peak of **2**.*

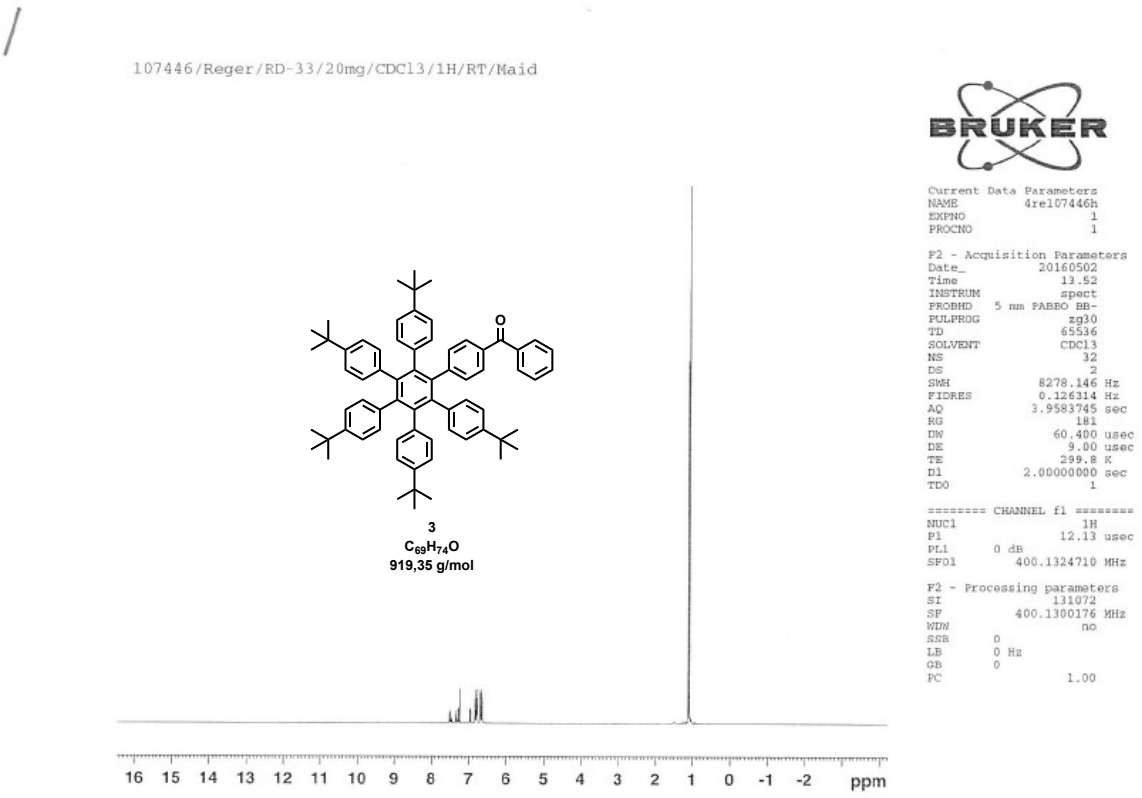

Figure S5: ^{1}H NMR spectrum of 3 ($CDCl_3$, 400 MHz; rt.).

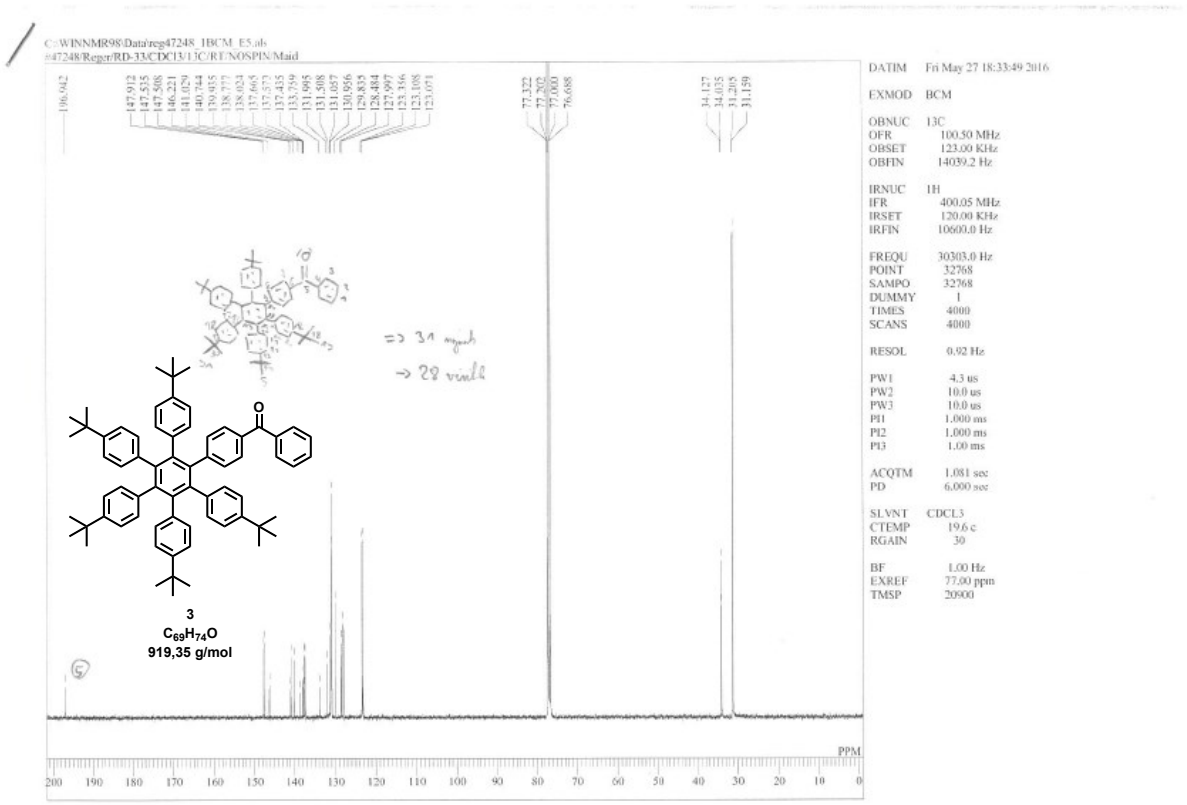

Figure S6: $^{13}C\{^{1}H\}$ NMR spectrum of 3 ($CDCl_3$, 100 MHz; rt.).

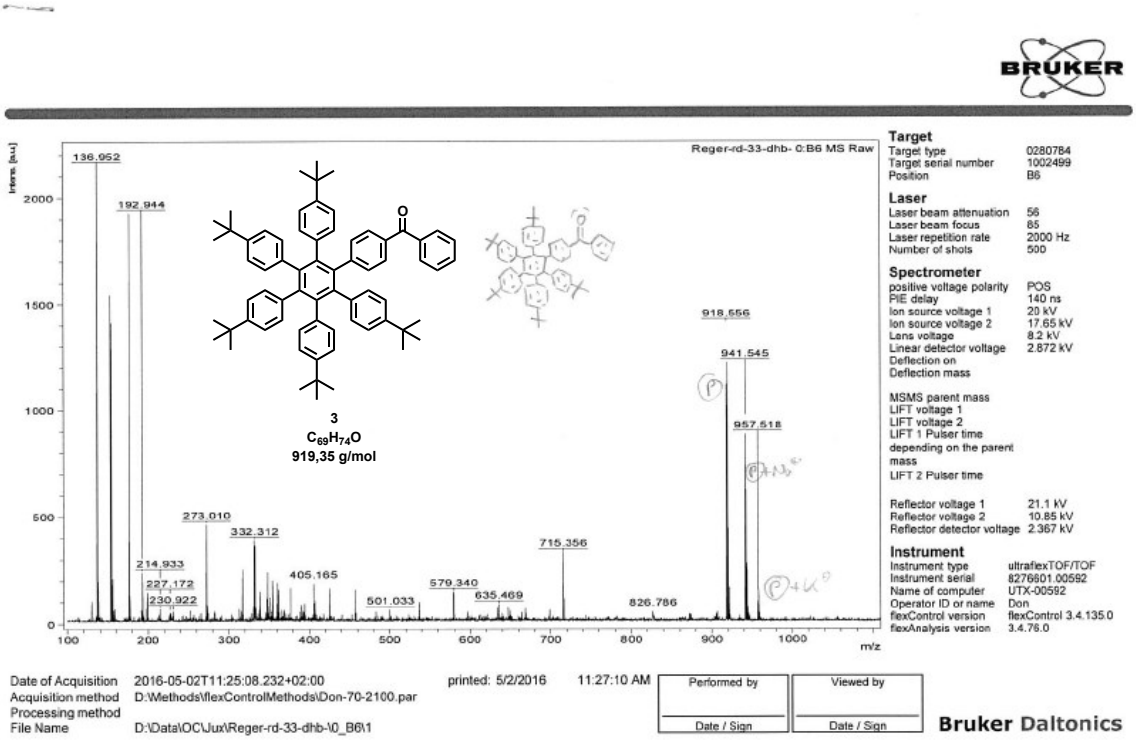

Figure S7: MALDI-ToF spectrum of 3 (dhb).

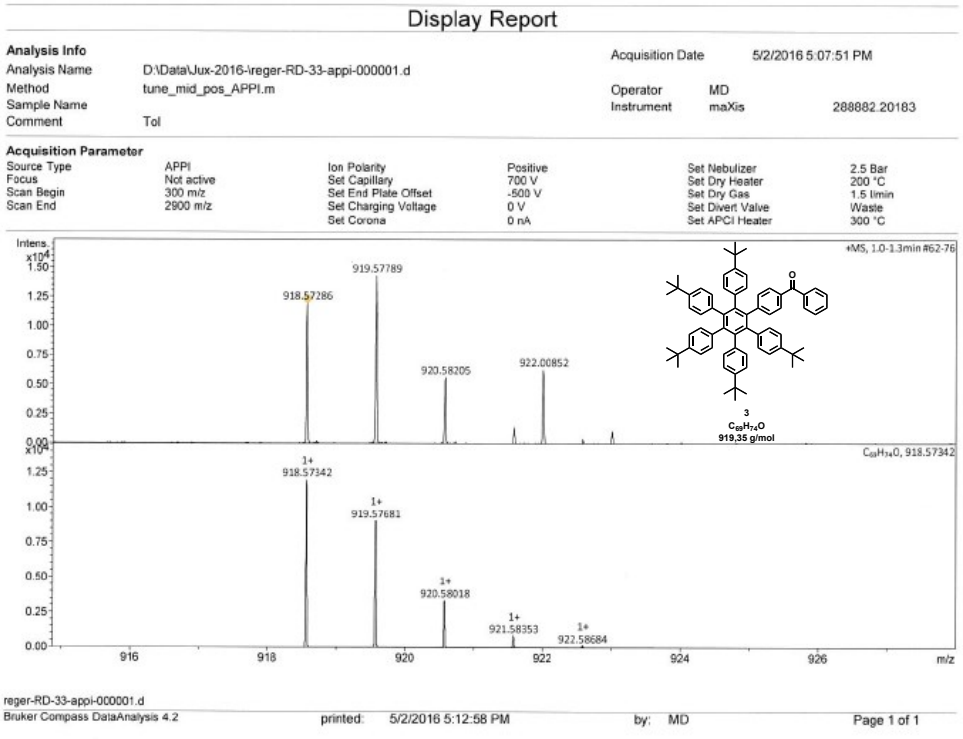

Figure S8: HRMS spectrum of 3 (APPI, toluene,). Top: Measured; Bottom: Calculated.

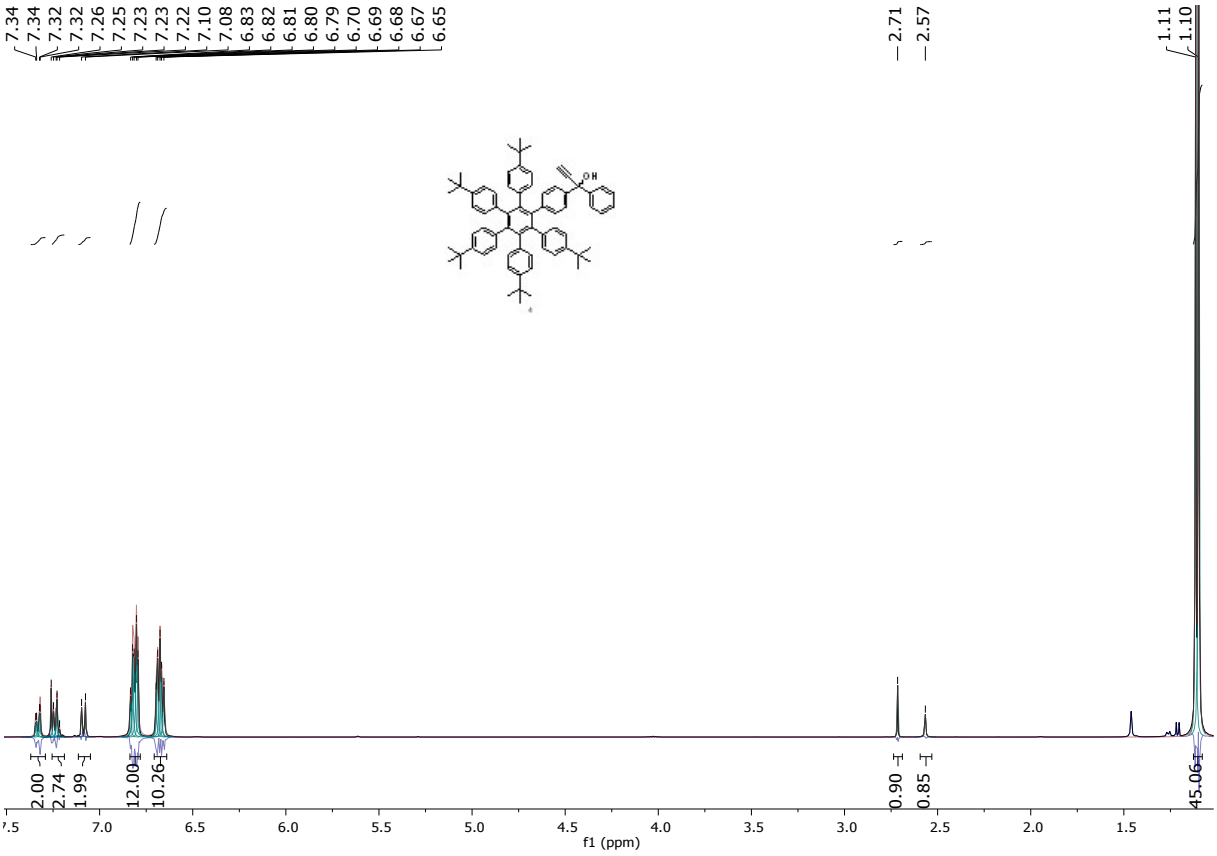

Figure S9: ^{1}H NMR spectrum of 4 ($CDCl_3$, 400 MHz; rt.).

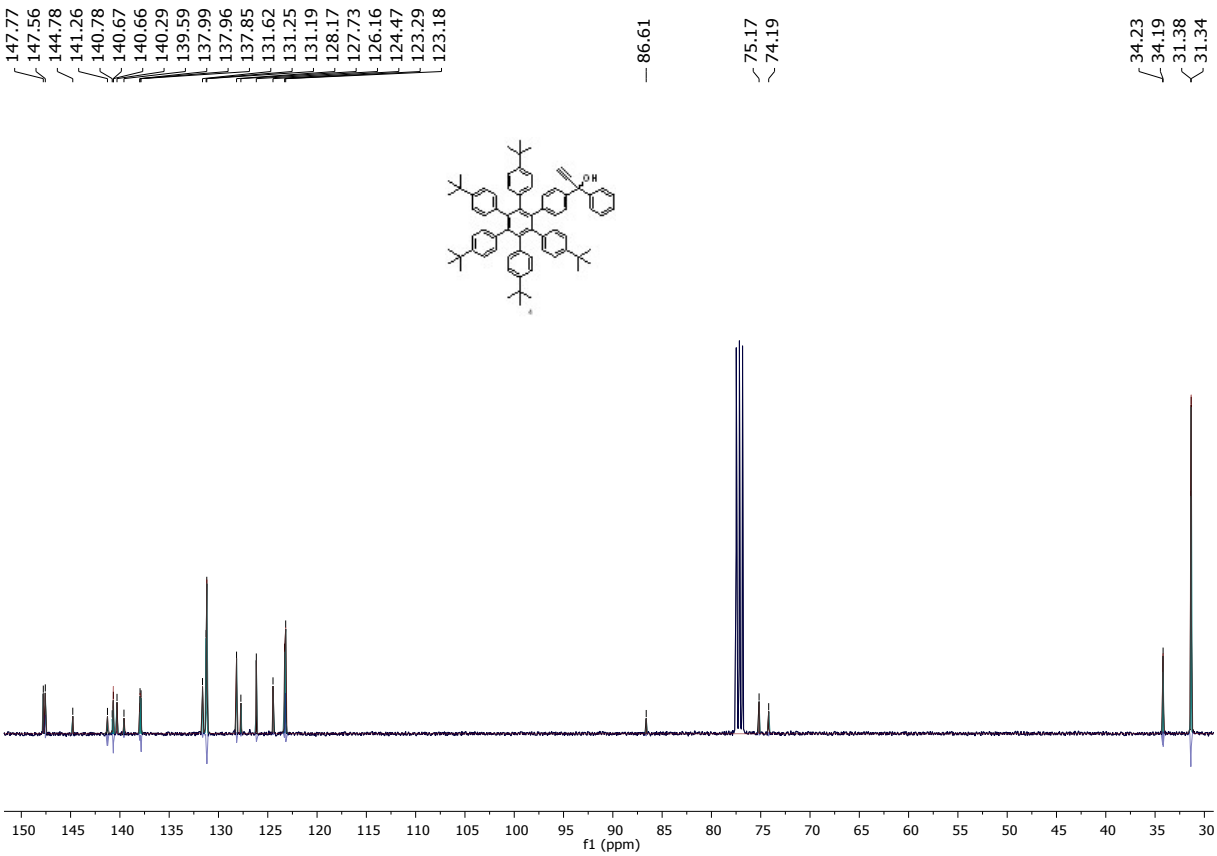

Figure S10: $^{13}C\{^{1}H\}$ NMR spectrum of 4 ($CDCl_3$, 100 MHz; rt.).

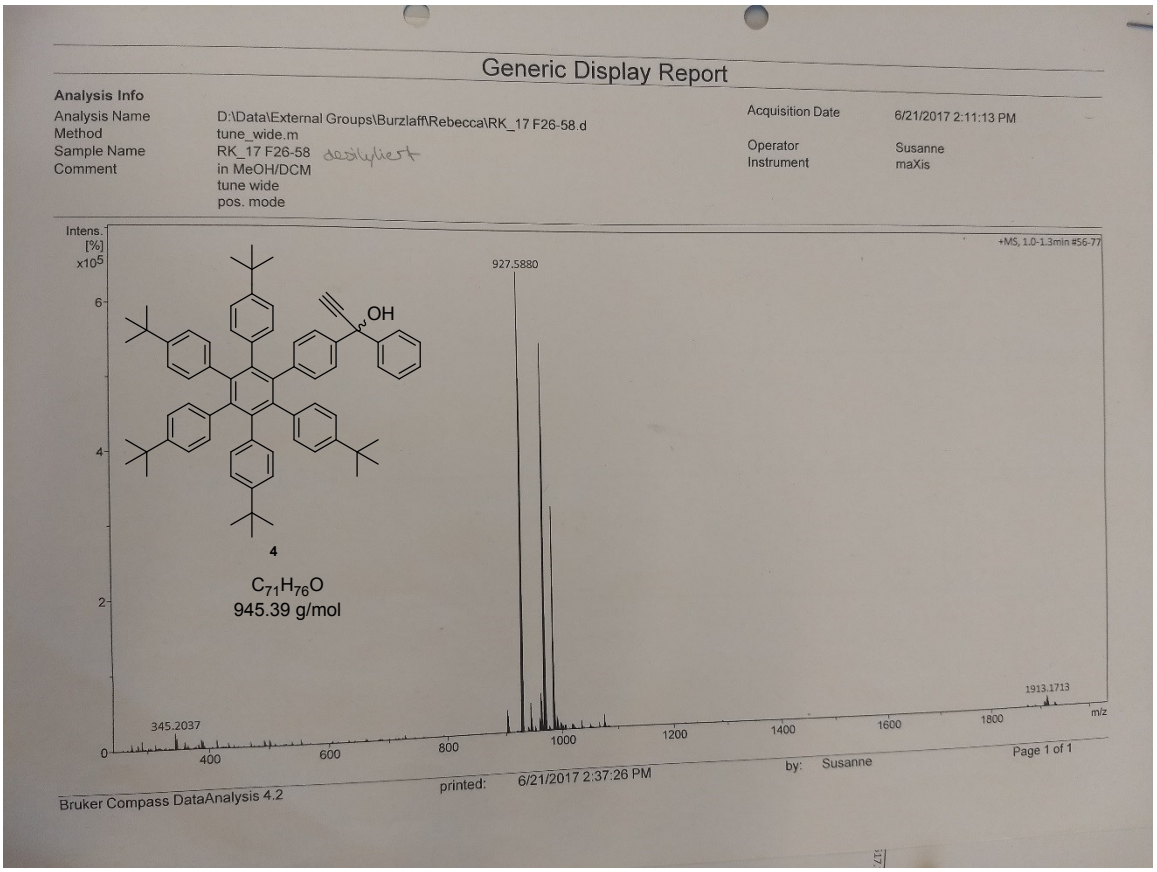

Figure S11: ESI-MS spectrum of 4

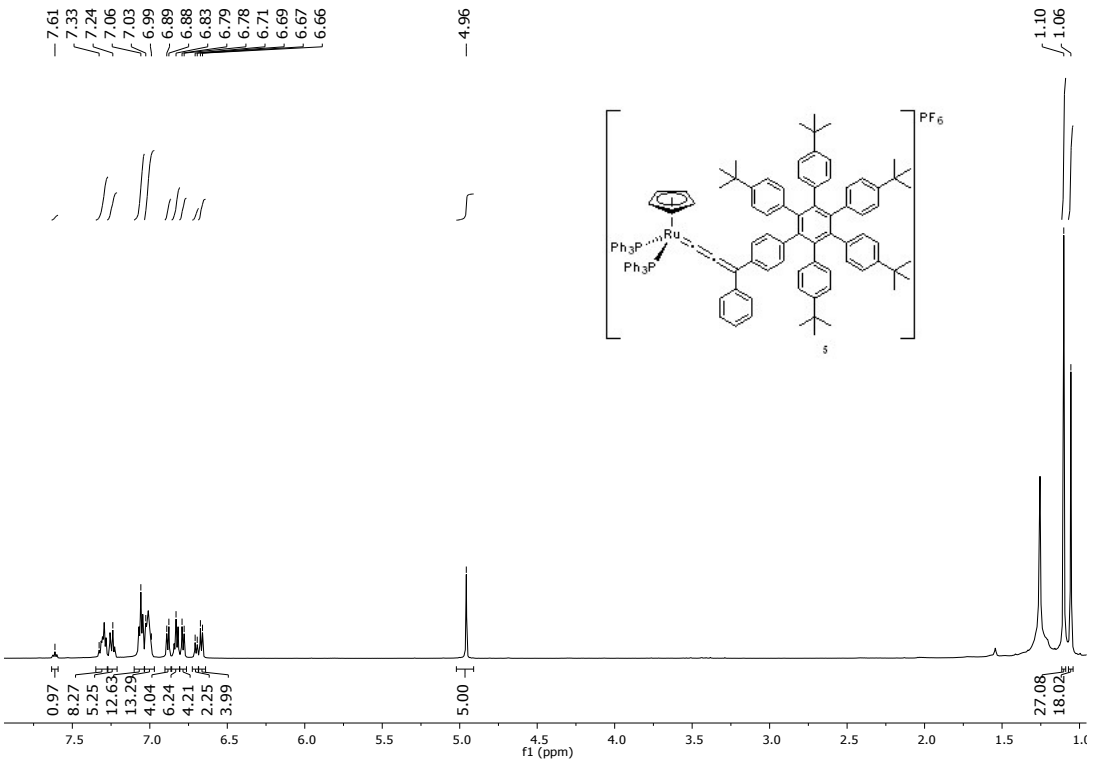

Figure S12: ^{1}H NMR spectrum of 5 (CD_2Cl_2, 600 MHz; rt).

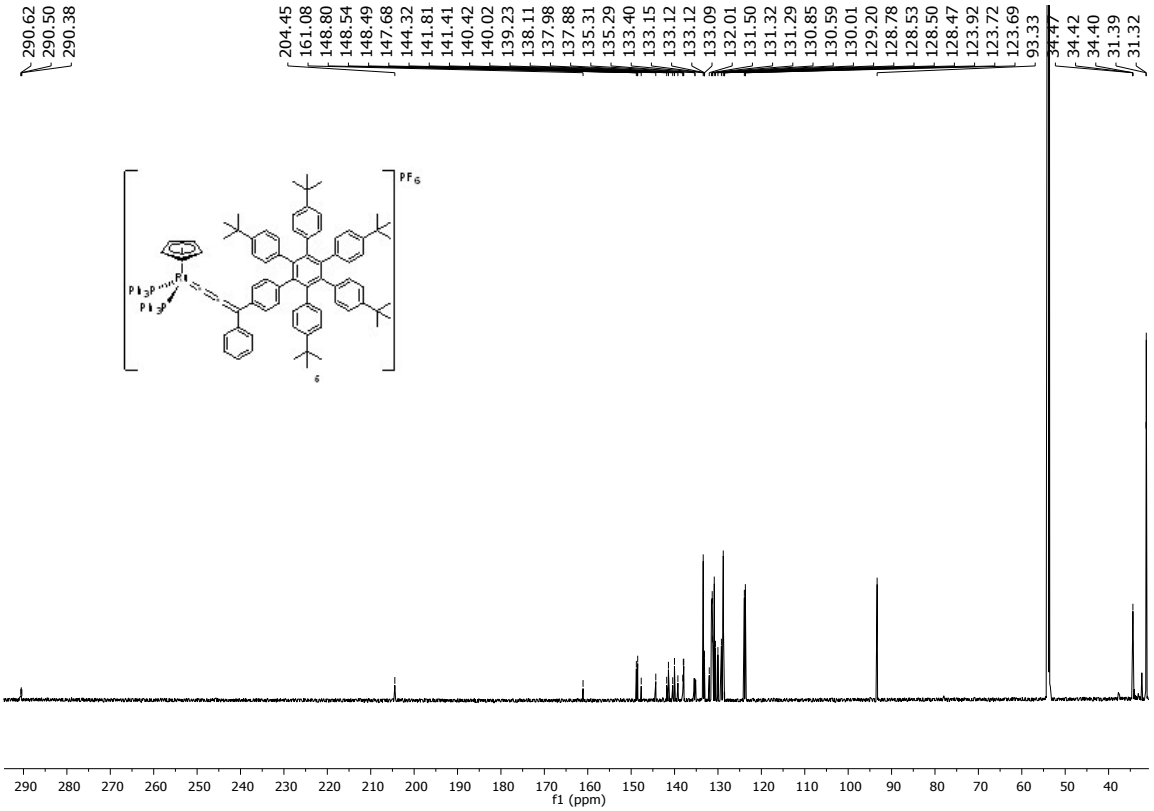

Figure S13: $^{13}C\{^{1}H\}$ NMR spectrum of 5 (CD_2Cl_2, 151 MHz; rt.).

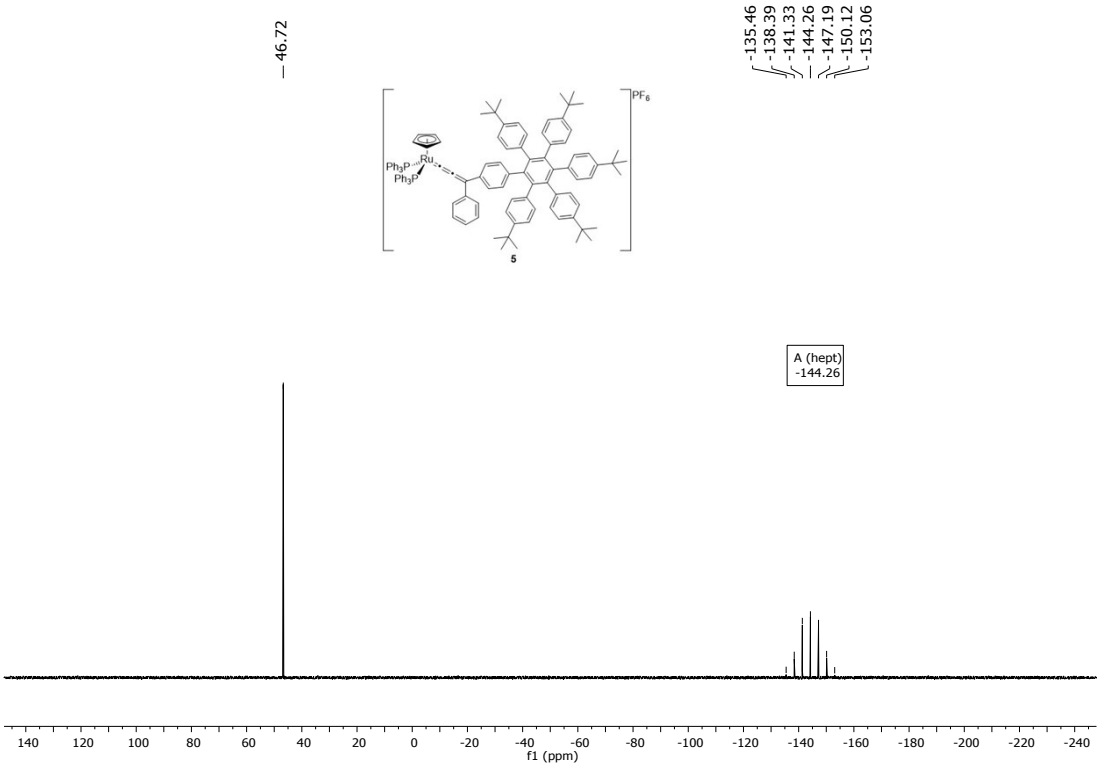

Figure S14: $^{31}P\{^{1}H\}$ NMR spectrum of 5 (CD_2Cl_2, 162 MHz; rt.).

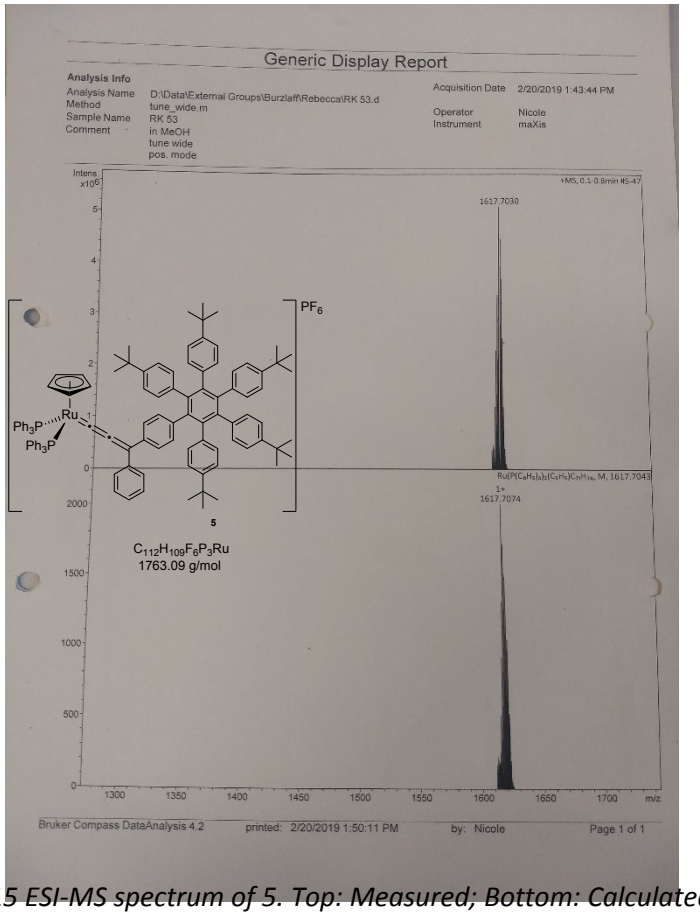

Figure S15 ESI-MS spectrum of 5. Top: Measured; Bottom: Calculated.

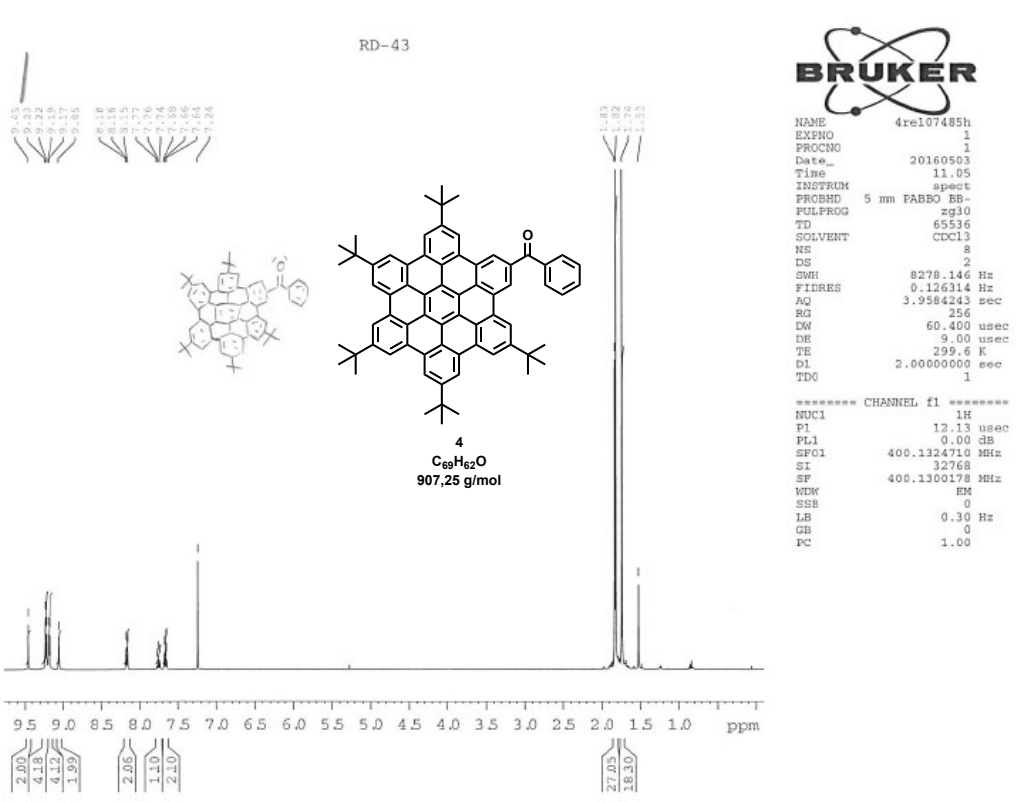

Figure S16: ^{1}H NMR spectrum of 6 ($CDCl_3$, 400 MHz; rt.).

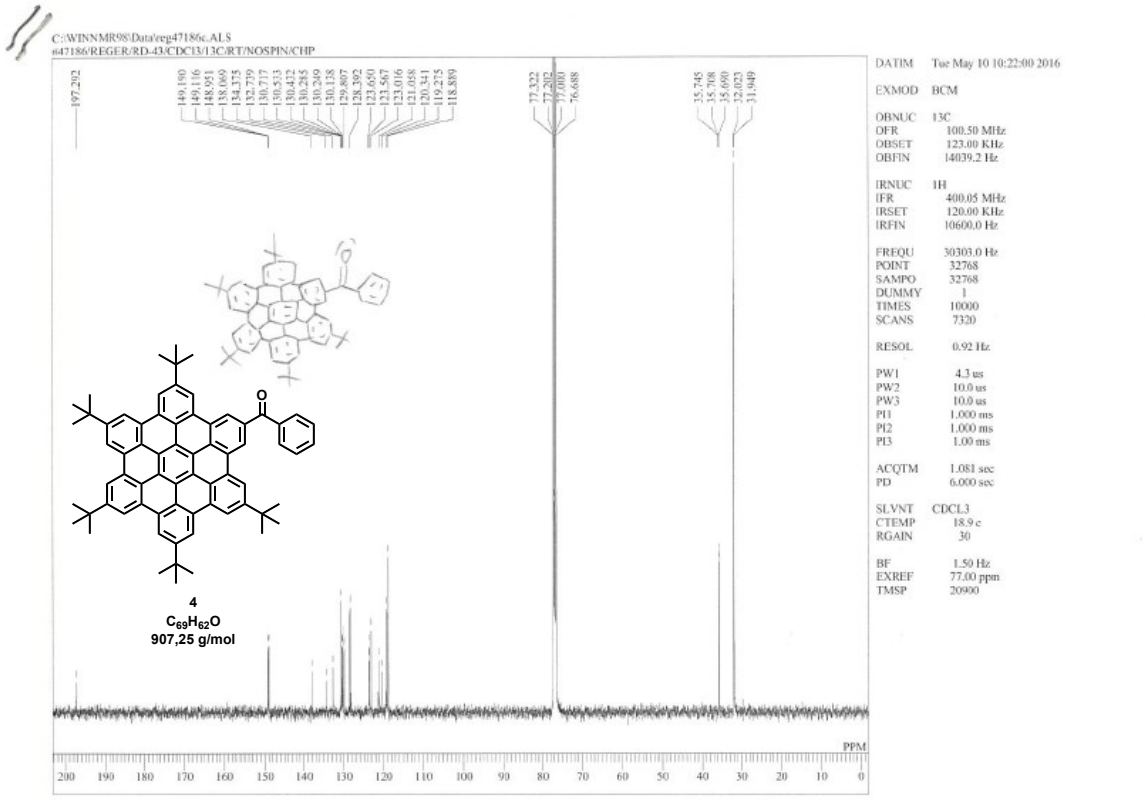

Figure S17: $^{13}C\{^{1}H\}$ NMR spectrum of 6 ($CDCl_3$, 100 MHz; rt.).

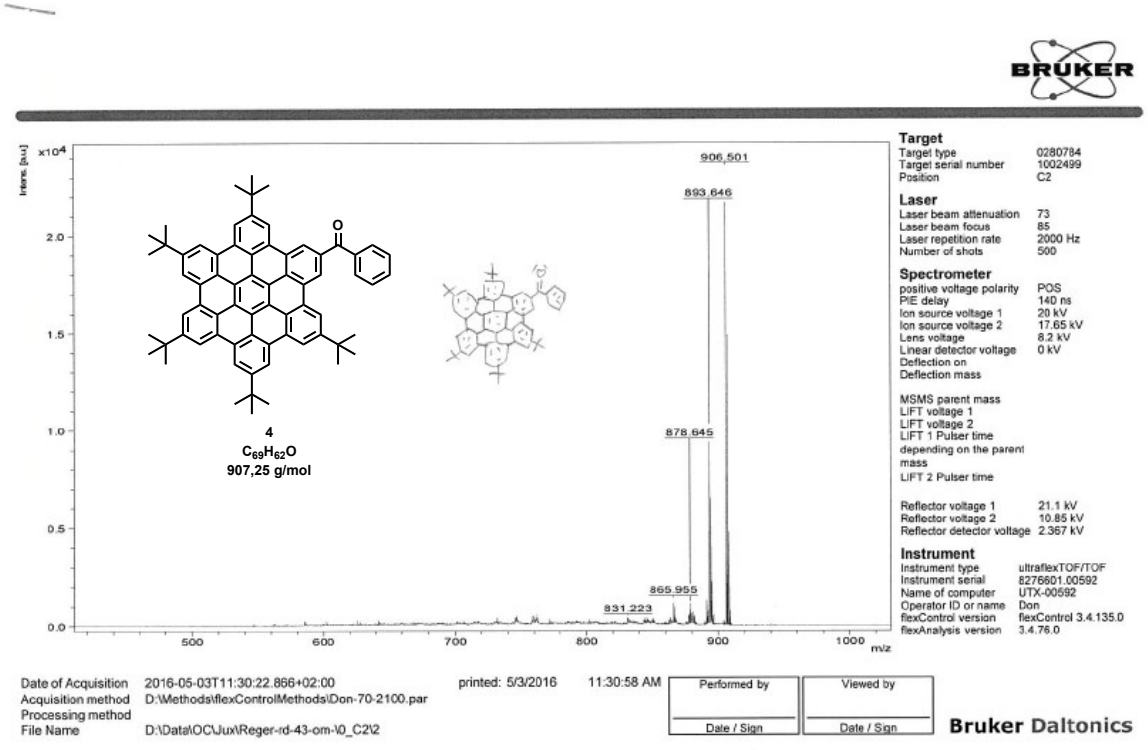

Figure S18: MALDI-ToF spectrum of 6 (om).

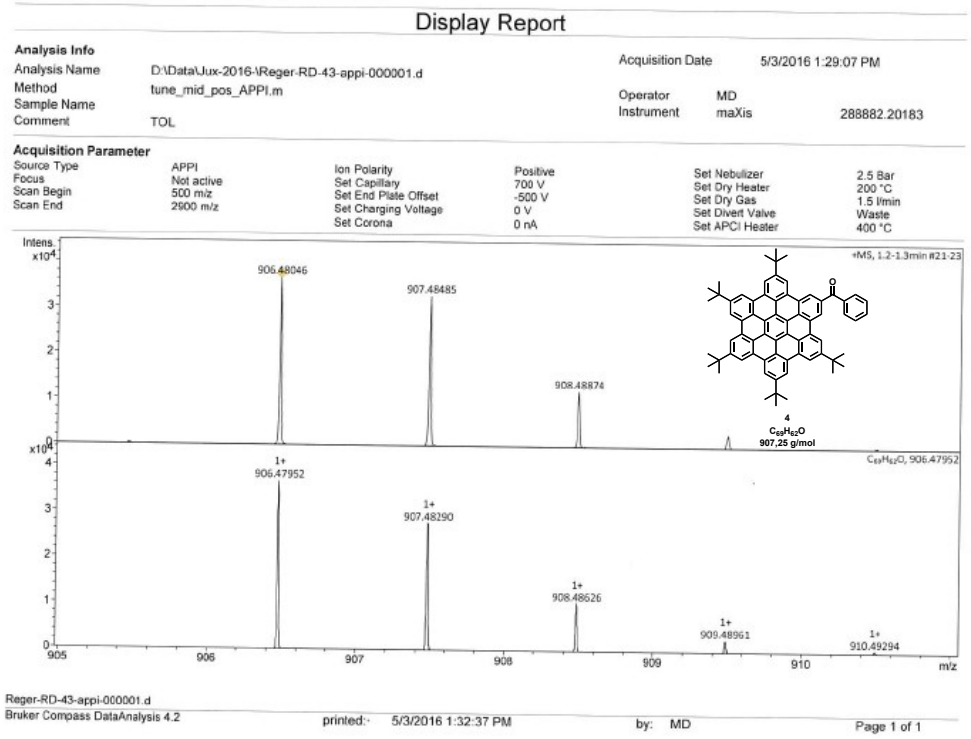

Figure S19: HRMS spectrum of 6 (APPI, toluene,). Top: Measured; Bottom: Calculated.

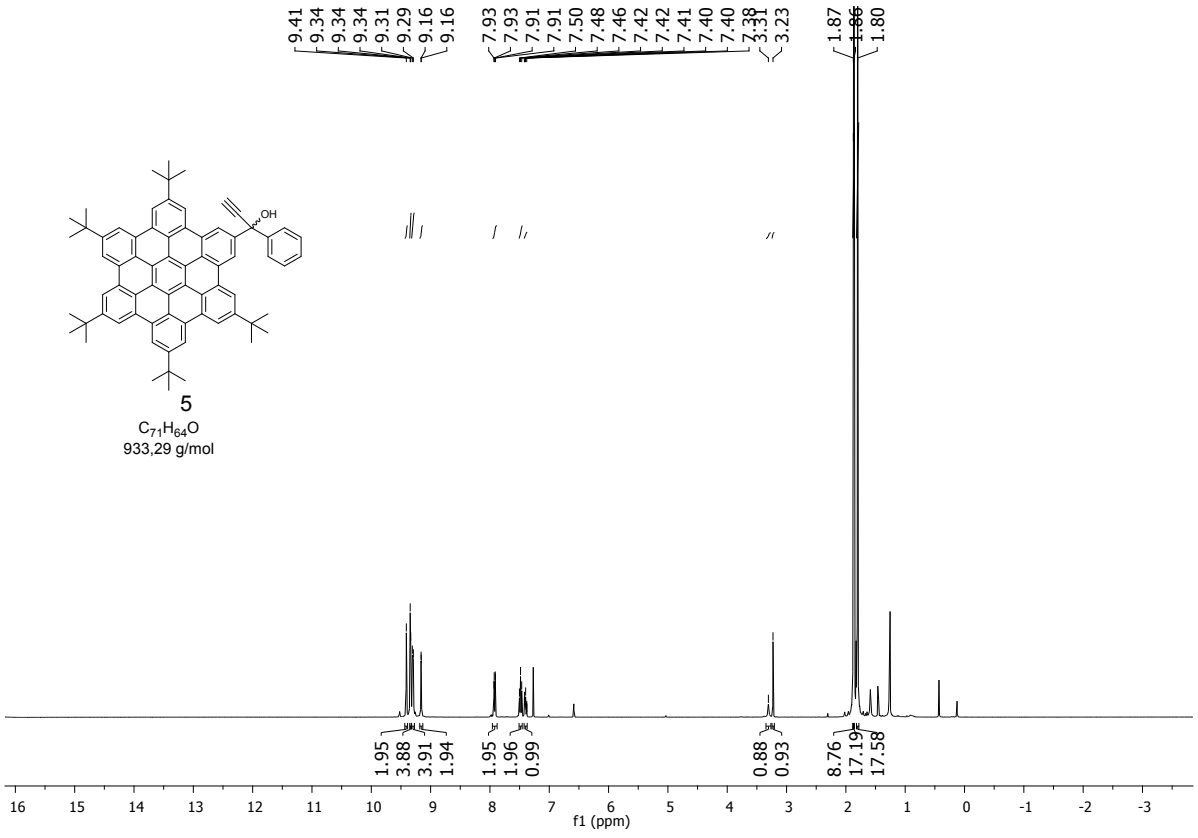

Figure S20: ^{1}H NMR spectrum of 7 ($CDCl_3$, 400 MHz; rt.).

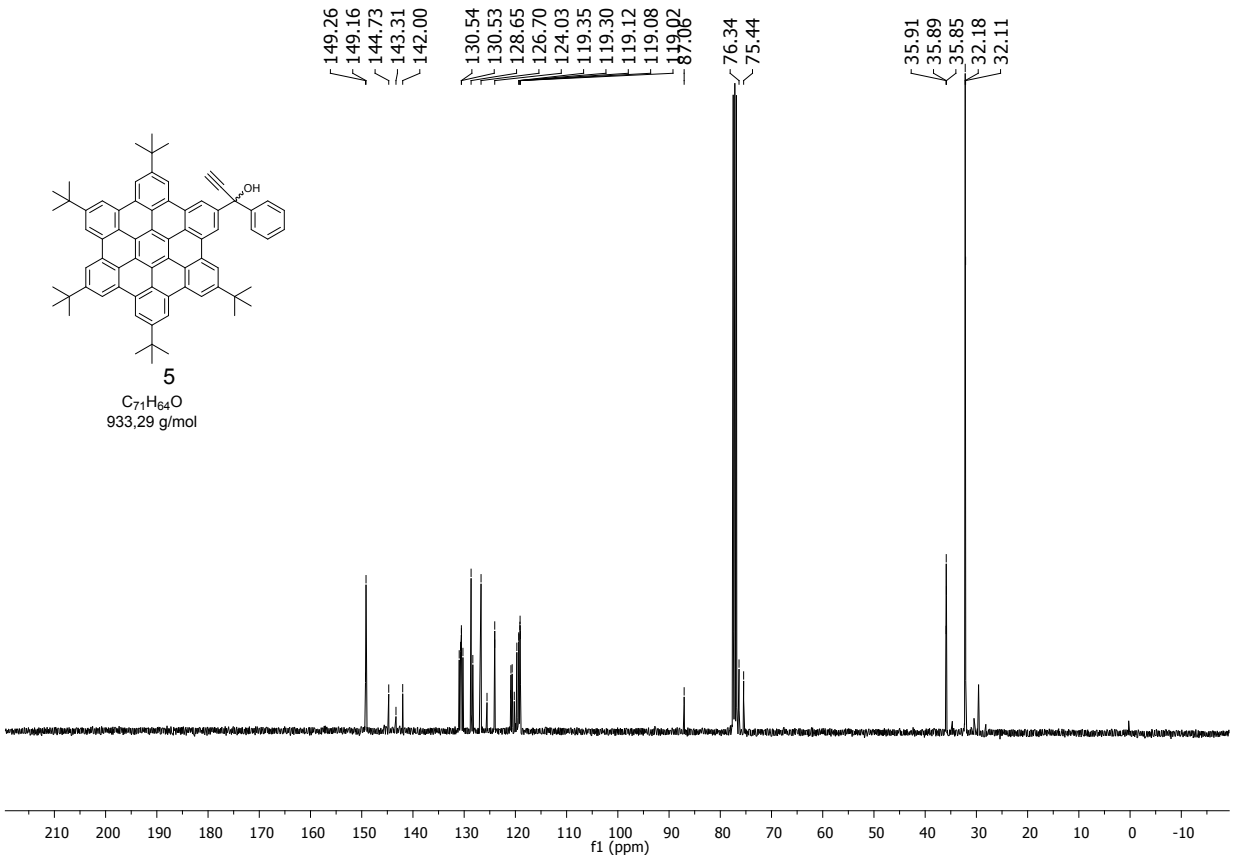

Figure S21: $^{13}C\{^{1}H\}$ NMR spectrum of 7 ($CDCl_3$, 100 MHz; rt.).

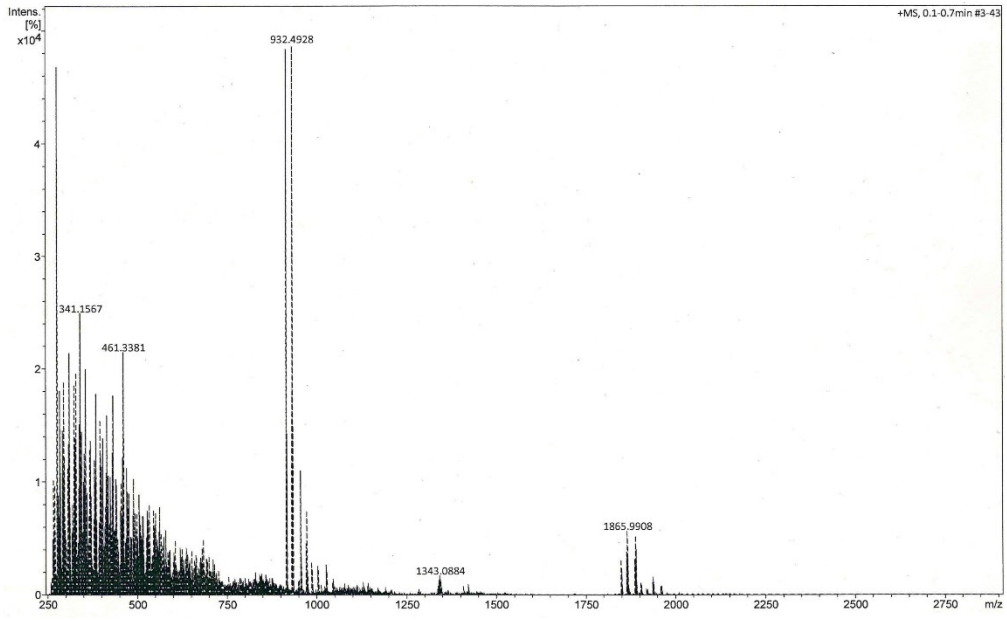

Figure S22: ESI-MS spectrum of 7.

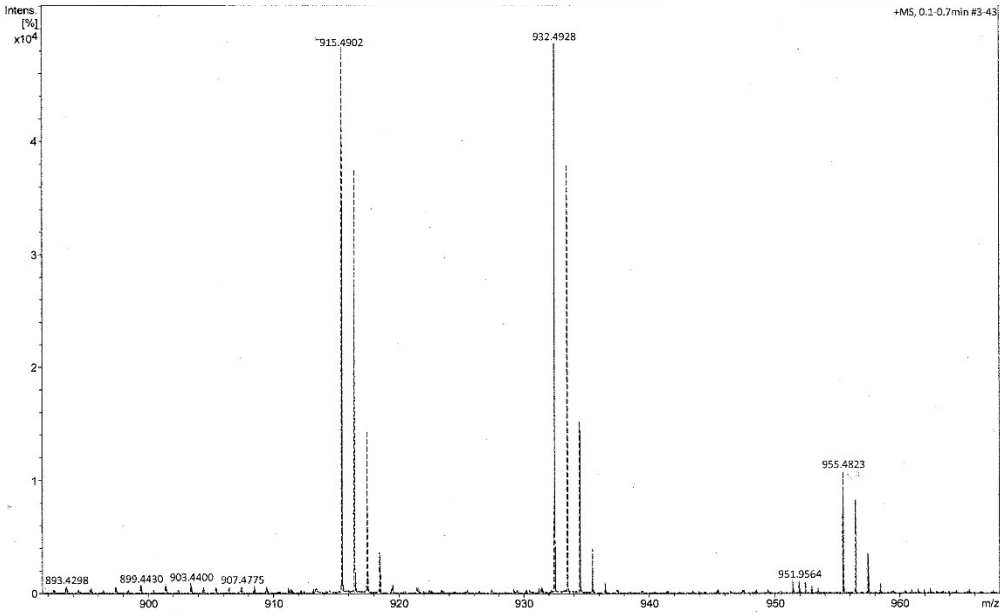

*Figure S23: ESI-MS spectrum of **7**.*

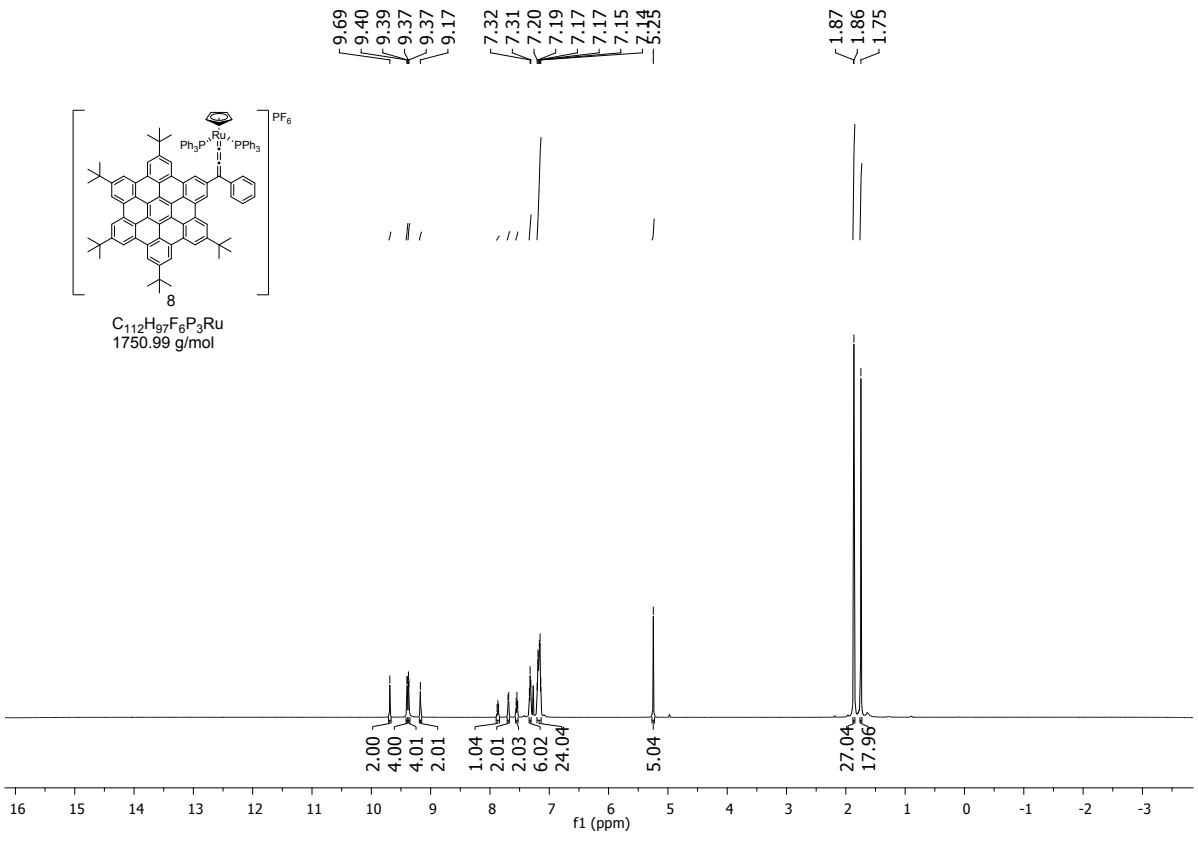

Figure S24: ^{1}H NMR spectrum of 8 ($CDCl_3$, 600 MHz; rt.).

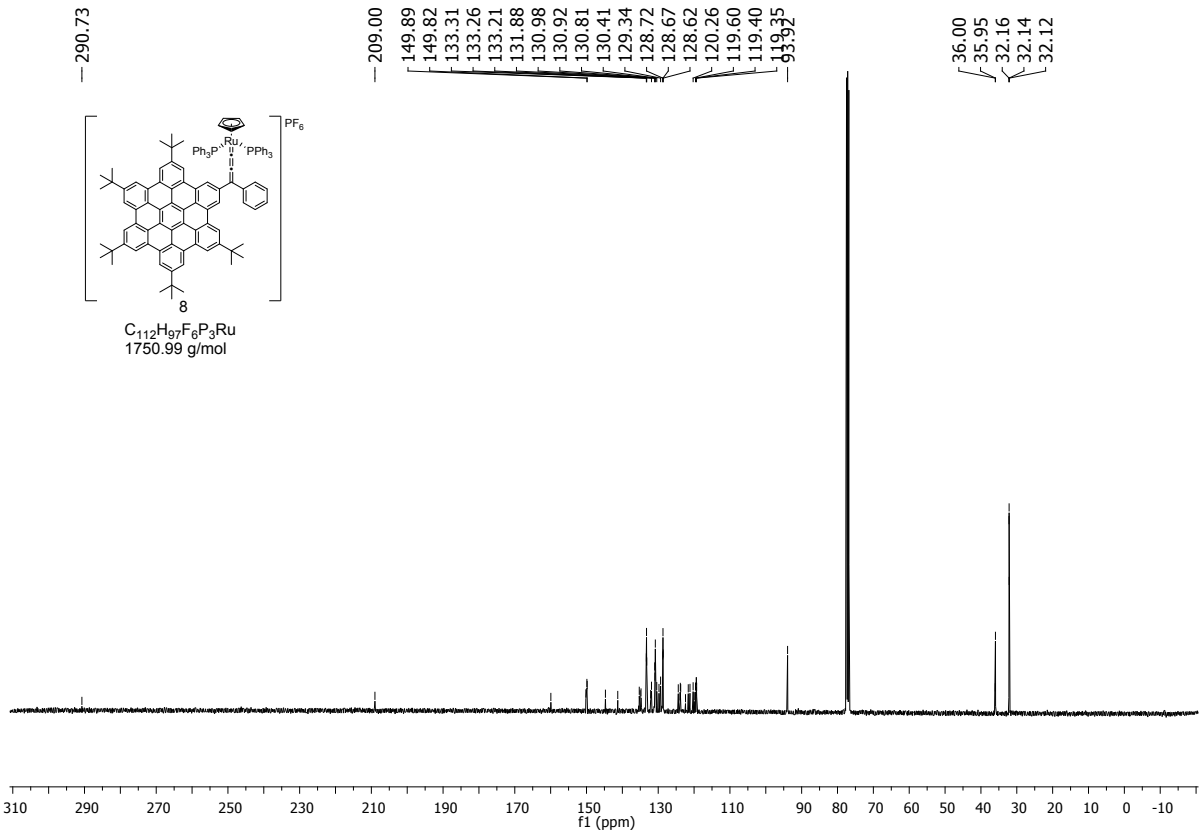

Figure S25: $^{13}C\{^{1}H\}$ NMR spectrum of 8 ($CDCl_3$, 151 MHz; rt.).

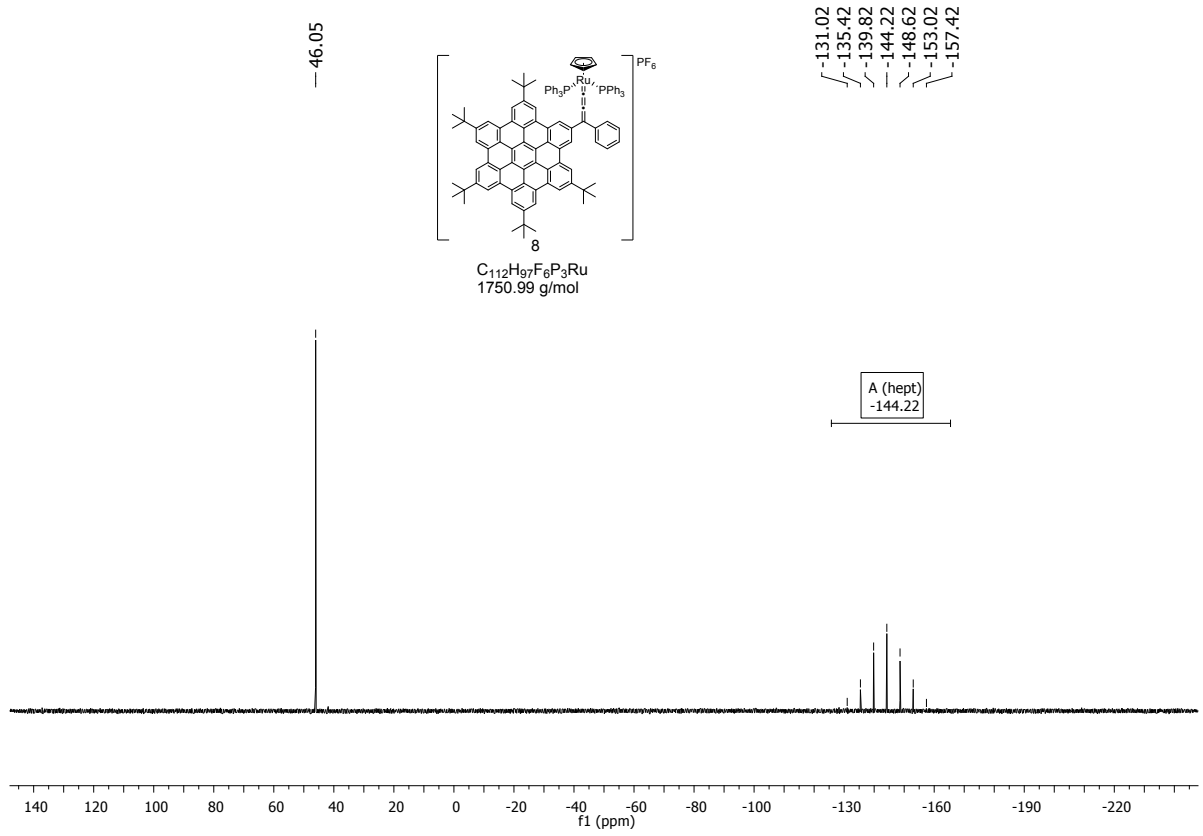

Figure S26: $^{31}P\{^{1}H\}$ NMR spectrum of 6 ($CDCl_3$, 162 MHz; rt.).

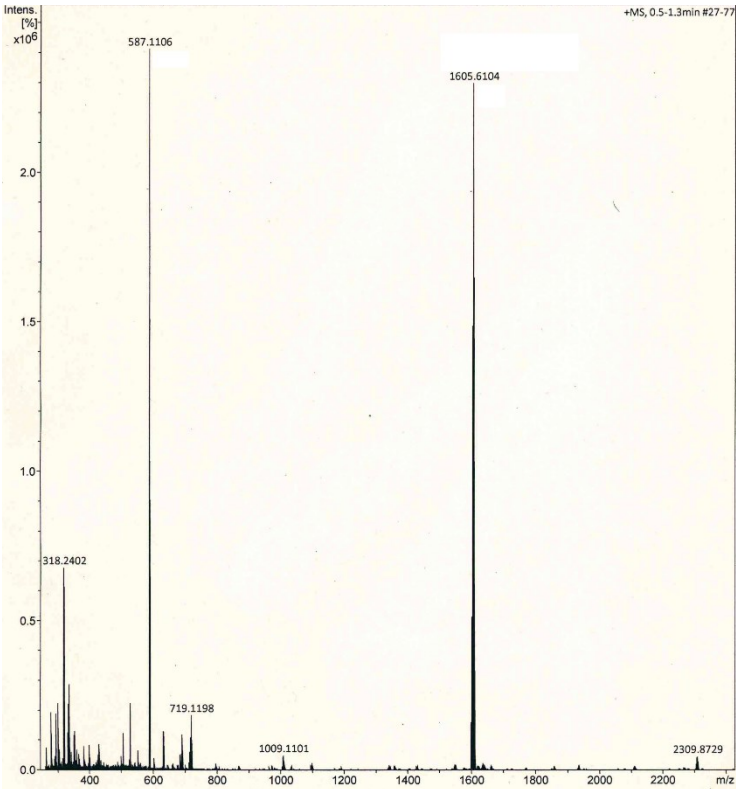

*Figure S27: ESI-MS spectrum of **8**.*

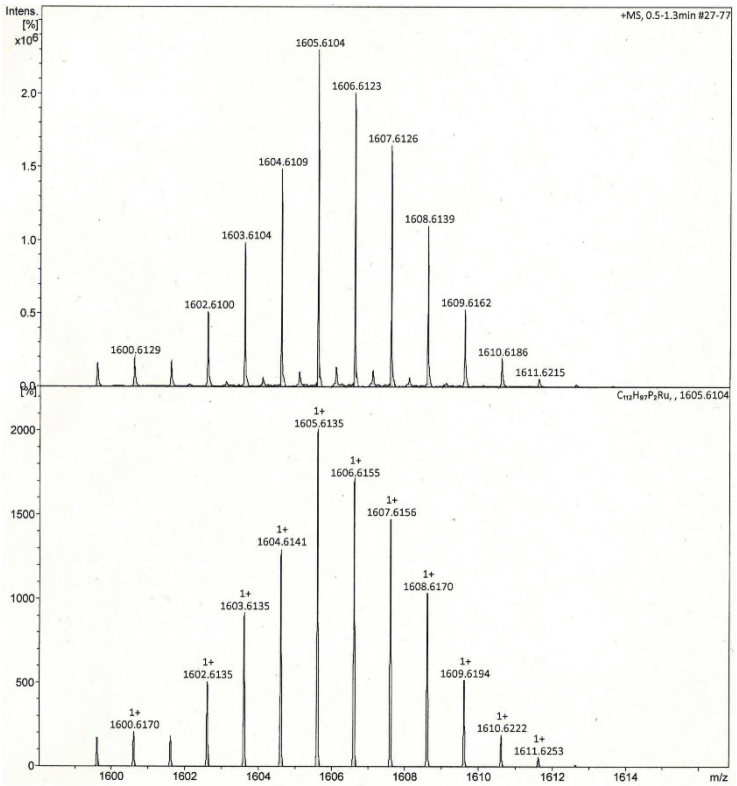

*Figure S28: ESI-MS spectrum of **8**. Top: Measured; Bottom: Calculated*

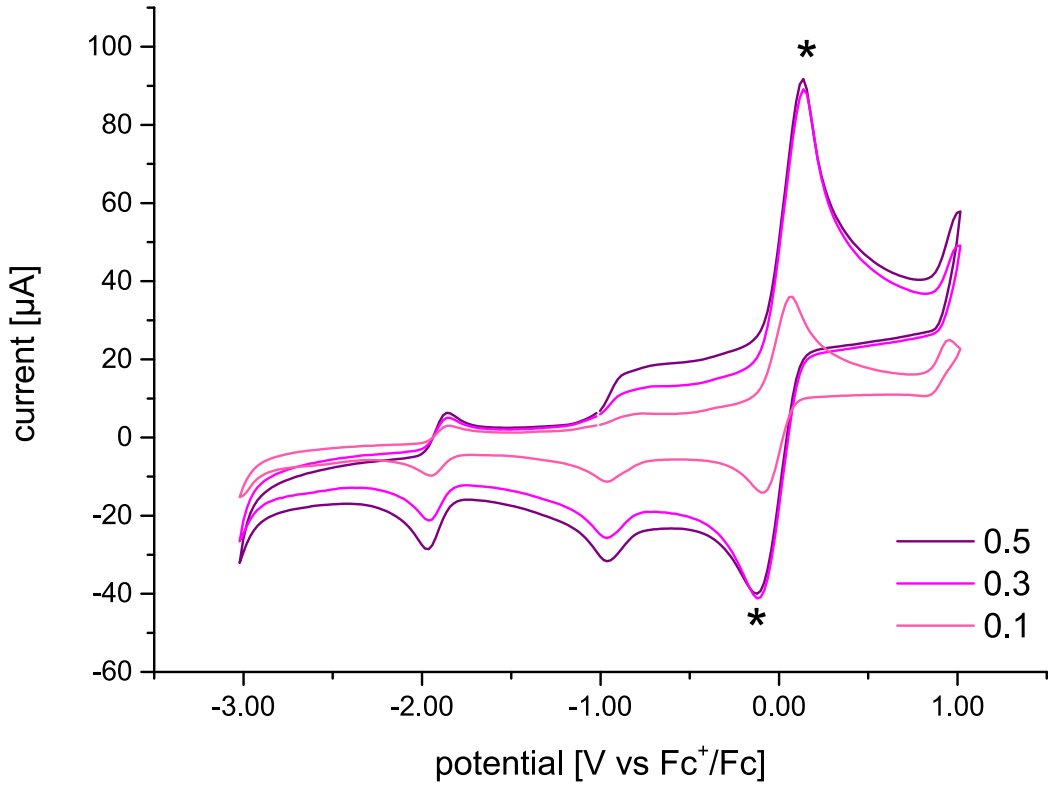

*Figure S29: Cyclic voltammograms of **5** (0.001 M) at different scan rates (0.1, 0.3 or 0.5 Vs^{-1}) on a Au electrode (0.1 V s^{-1}, 0.2 M n-Bu_4NPF_6/CH_2Cl_2, referenced to internal Fc^+/Fc). * marks the redox sweep of the Fc^+/Fc reference redox couple.*

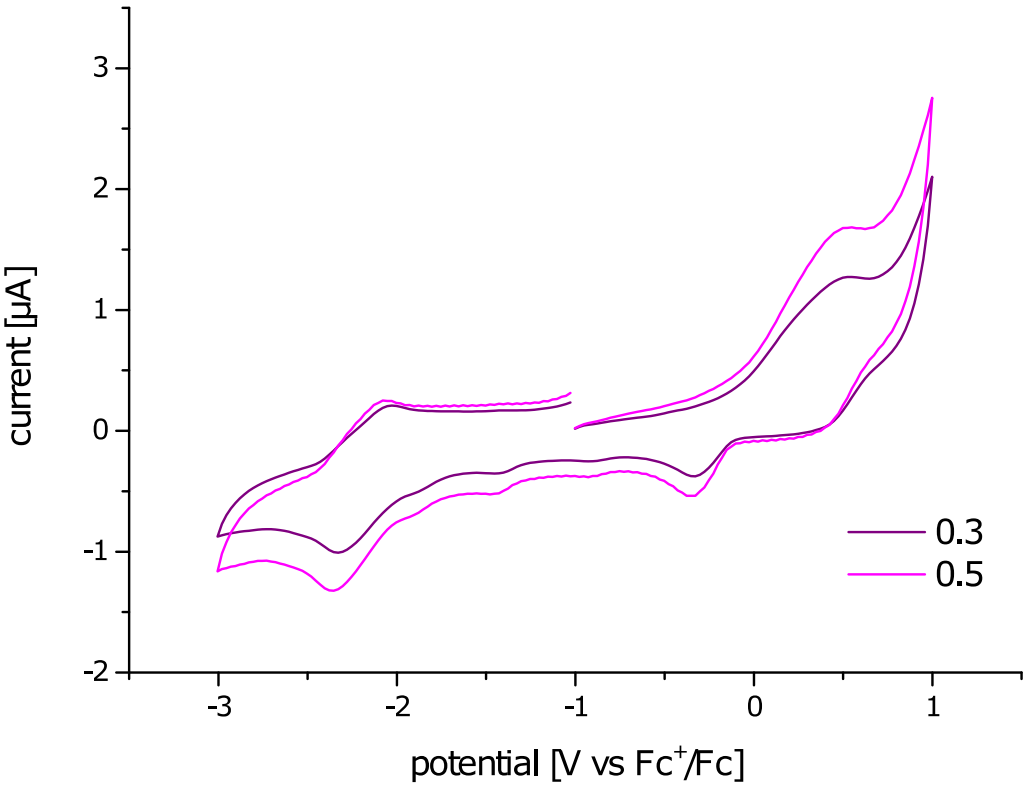

*Figure S30: Cyclic voltammograms of **5** (0.001 M) at different scan rates (0.3 or 0.5 Vs^{-1}) on a Au electrode (0.1 V s^{-1}, 0.2 M n-Bu_4NPF_6/CH_2Cl_2, without internal Fc^+/Fc).*

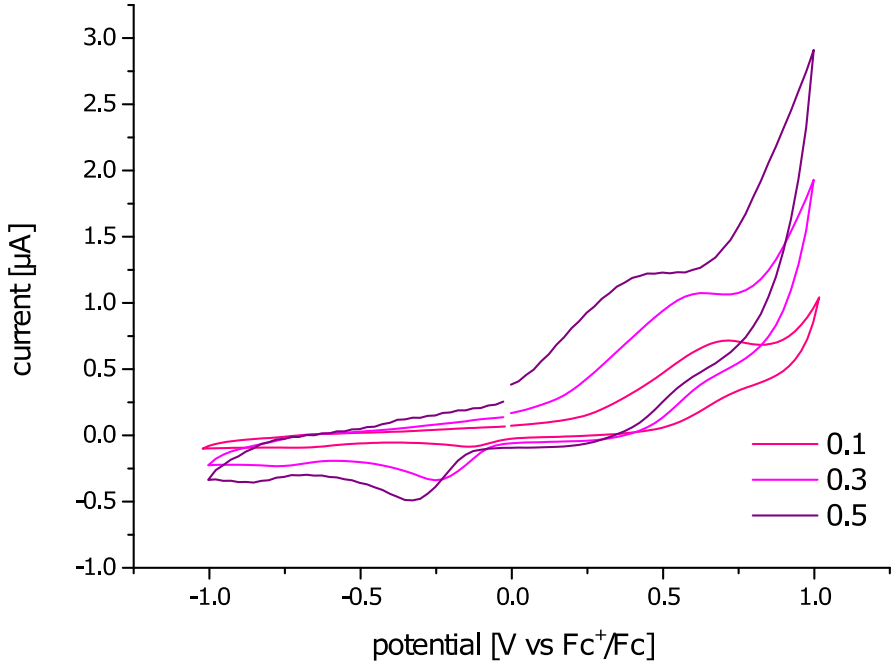

*Figure S31: Cyclic voltammograms of **5** (0.001 M) at different scan rates (0.1, 0.3 or 0.5 Vs^{-1}) on a Au electrode (0.1 V s^{-1}, 0.2 M n-Bu_4NPF_6/CH_2Cl_2, without internal Fc^+/Fc).*

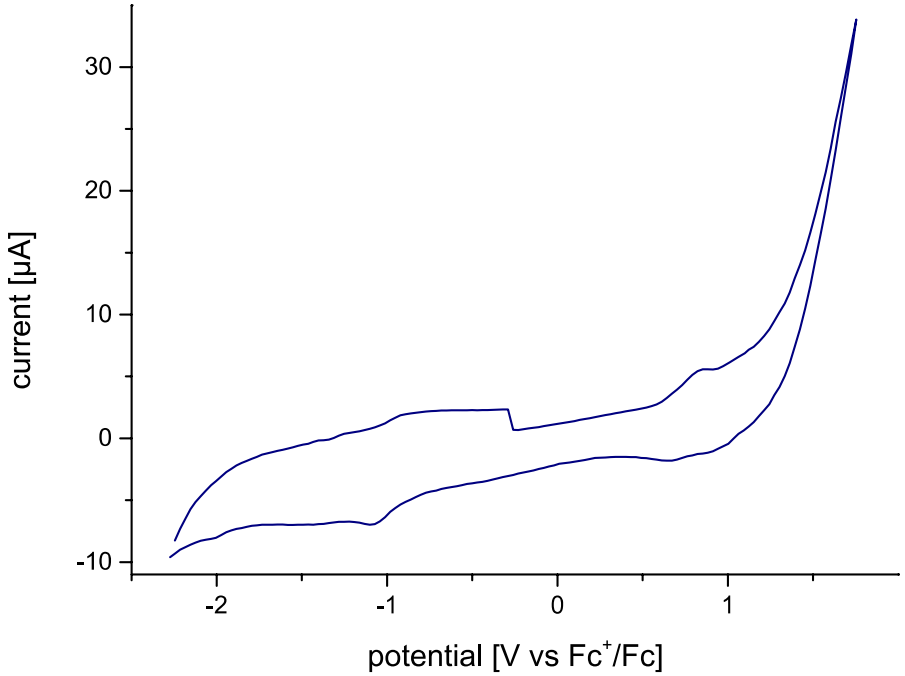

*Figure S32: Cyclic voltammogram of **8** (0.001 M) at a scan rate of 0.5 Vs^{-1} on a Au electrode (0.1 V s^{-1}, 0.2 M n-Bu_4NPF_6/CH_2Cl_2, without internal Fc^+/Fc).*

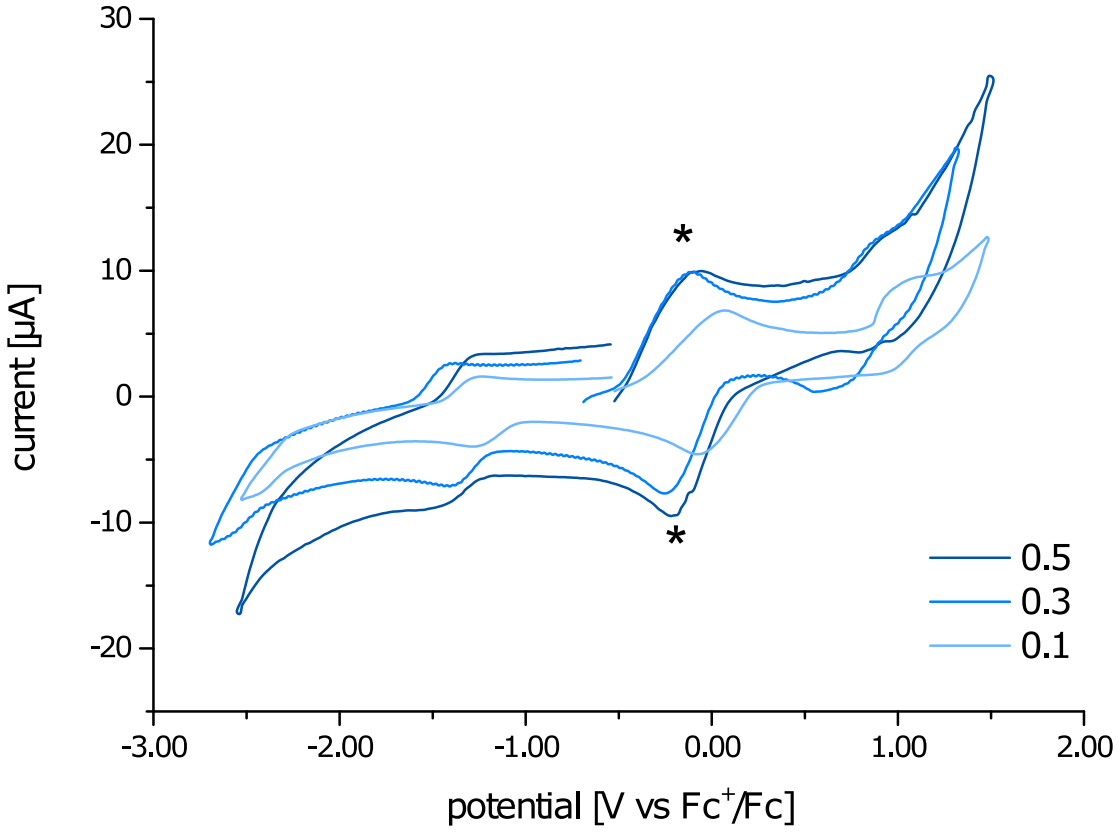

*Figure S33: Cyclic voltammograms of **8** (0.001 M) at different scan rates (0.1, 0.3, 0.5 Vs^{-1}) on a Au electrode (0.1 V s^{-1}, 0.2 M n-Bu_4NPF_6/CH_2Cl_2, referenced to internal Fc^+/Fc). * marks the redox sweep of the Fc^+/Fc reference redox couple.*

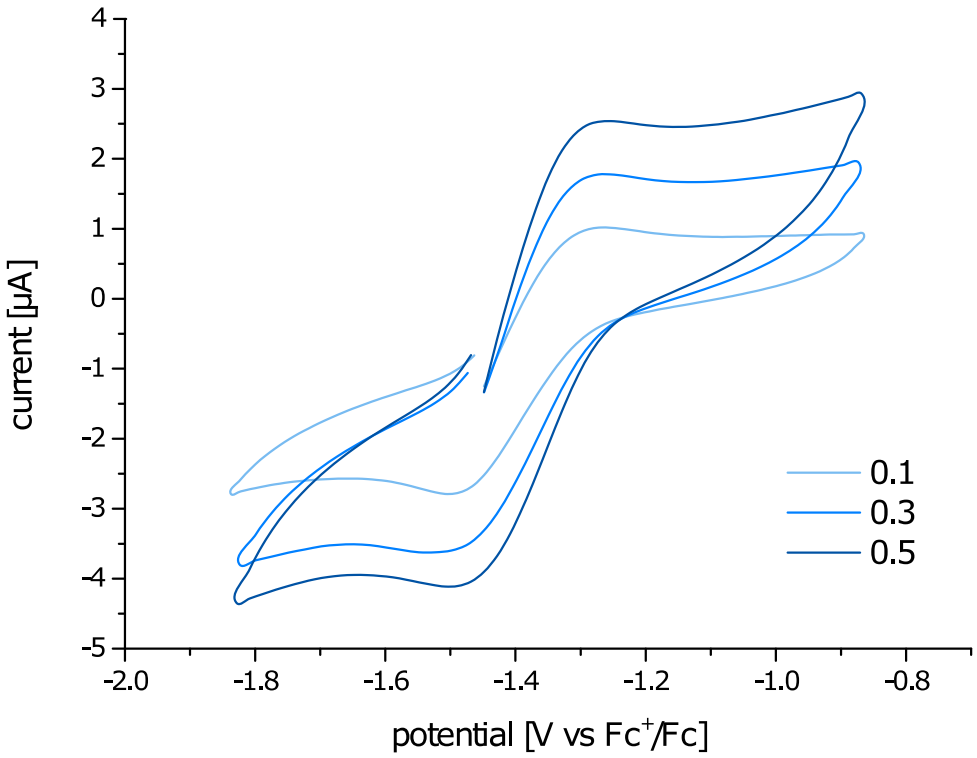

*Figure S34: Cyclic voltammograms of **8** (0.001 M) at different scan rates (0.1, 0.3, 0.5 Vs^{-1}) on a Au electrode (0.1 V s^{-1}, 0.2 M n-Bu_4NPF_6/CH_2Cl_2, referenced to Fc^+/Fc).*